

Image Retrieval based on the Fusion of Graph Method with Color Moments, GLCM, and Hu Moments

Akmal^{a,b,*}, Rinaldi Munir^a, Judhi Santoso^a

^a School of Electrical Engineering and Informatics, Institut Teknologi Bandung, Jl. Ganeca 10, Bandung, 40132, Indonesia

^b Department of Computer Science, Universitas Padjadjaran, Jl Raya Bandung-Sumedang km 21, Jatinangor, 45363, Indonesia

Corresponding author: *akmal@unpad.ac.id

Abstract—Retrieving images that are similar to the query image in the image database means determining the similarity between the images. This study aims to use a graph method with region adjacency graph representation in conjunction with a non-graph method in image retrieval. We represented an image as a graph and used the Graph Edit Distance (GED) method to calculate the similarity between two graphs. The feature extraction of the image graph, which exposes the content and the relationships between existing content, is a key step in image retrieval based on the graph method. The extraction of graph features is accomplished by the image segmentation method, which divides the image into regions and represents them as a region-adjacency graph (RAG), in which vertices represent regions and edges indicate two neighboring regions. Image retrieval based on the graph method is combined with low-level approaches like Color Moments, Gray Level Co-occurrence Matrix (GLCM), and Hu Moments to boost accuracy. All obtained features are normalized, weighted, and then compared between images to get the similarity value using Euclidean Distance. An image retrieval prototype based on the combined graph method and non-graph method was successfully created in this work, using four datasets: synthetic, batik, COIL-100, and Wang. The MAP of the four datasets is 67.84 percent, but when combined with the low-level feature approach, it rises to between 79.73 and 89.71 percent. The combination of graph and non-graph algorithms improves image retrieval outcomes.

Keywords— Region adjacency graph; graph edit distance; color moment; gray level co-occurrence matrix; Hu moment.

Manuscript received 30 Mar. 2022; revised 13 Jan. 2023; accepted 21 Mar. 2023. Date of publication 30 Jun. 2023.
IJASEIT is licensed under a Creative Commons Attribution-Share Alike 4.0 International License.



I. INTRODUCTION

Recently, gigabytes of images have been generated daily and grown exponentially. As a result, finding relevant information from image databases becomes an important and challenging task. Content-based image retrieval aims to search images in huge databases based on visual image content efficiently and accurately according to user needs [1]. Extraction carried out by traditional pixel-based methods is ineffective because it only represents the content. The approach of extracting graphs from images is very promising, although it is not easy. Extraction of this graph is an important stage in image analysis using graphs and becomes the basis for processing at a later stage [2].

The graph is a popular data structure consisting of graph vertices representing entity information and graph edges representing binary relationships between entities. Graph representations have been used for pattern recognition in image objects, documents, e-mail, 2D and 3D shapes,

characters, and symbols. In addition, they are also used in semantic web content, social networks, chemical or biological structures, economics, and many more [3]. Meanwhile, Sun et al. [4] stated in their survey that graph matching has been widely used in many applications that use correspondence, such as object detection, face recognition, object tracking, robotics, image registration, and action recognition.

The reasons for using graph-based image processing and analysis are that it is suitable for developing efficient methods because of its simplicity of representation, and it has the flexibility to represent many different types of images. It is possible to redevelop algorithms and theorems from graph theory so that they can be used in image analysis. The increasing performance, representation, and ability to understand semantic aspects are the things that cause the growing image retrieval approach using graph theory [5]. Image retrieval techniques have been widely researched to obtain efficient techniques, but currently, there are no universally available techniques for image extraction, indexing, and retrieval. Therefore, this is still a problem that

continues to be explored and, at the same time, has become a field of study that is still being actively pursued [6]. Hameed et al. [7] conducted a survey, analysis, and compared the latest methodologies in the CBIR field in the 2015-2020 interval, which inspired further research in the CBIR field. Amit K. Nath specifically explored image retrieval techniques in photo organizer applications [8]. Meanwhile, Tena et al. [9] conducted a study on applying feature extraction methods for fabric images, which were divided between conventional techniques and convolutional neural networks.

The graph-matching problem is related to discrete combinatorial optimization, a basic problem in computer vision and pattern recognition to find the correspondence of nodes between two or more graphs [10]. Sharma et al. proposed a new method for CBIR through graph-theoretical matching using inexact graph-matching techniques based on tree search by determining the similarity between histological images [11]. Kumar et al. [12] proposed using the Vector Space Embedding method to find the similarity between two graphs in Graph-Based Retrieval of PET-CT Images. Luo and Xu [13] proposed a region-matching algorithm using consistency and region adjacency graphs to compare two images. Valdes-amaro and Lopez-prieto [14] introduced a new technique using global features with interest point detection and Delaunay triangulation to form graphs which were then searched for similarities. Kashif et al. [15] perform Diagnosis of Lung Diseases based on comparing the similarity of visual features and graph-based similarity comparison of balanced graphs. Selective Rank Fusion, a graph-based technique described by Valem and Pedronette [16], is utilized to depict the estimation of feature efficacy and complementarity. Meanwhile, Cortes et al. [17] bring the potential of machine learning into an Edit Distance Graph (GED), which presents a framework used to estimate the value of the edit cost for node substitution.

Low-level features like color, shape, and texture are particularly prevalent in CBIR [18]. Using visual image information such as color, shape, and texture in image representation and indexing is difficult in finding and retrieving images from database collections [19]. However, much work is still being done to obtain an effective and efficient CBIR process model. Alsmadi [20] employs color, shape, and texture descriptors and features in his CBIR system. By combining features from the random forest classifier, color, greyscale, shape, and texture, Subramanian proposed a method to improve the effectiveness and efficiency of the CBIR system. He employed the Particle Swarm Optimization algorithm to choose useful features [21]. Singh and Batra [22] described a two-layer image retrieval method that compares the query images in the texture and shape space before comparing the M-resulting images with the shape and color feature spaces to yield F-resulting images. Vimina and Divya [23] proposed a technique to overcome the problem of high-dimensional image feature vectors using texture and color descriptors by integrating multi-channel features in CBIR.

Khan et al. [24] proposed a hybrid framework in the CBIR method in a multi-class scenario using feature extraction from color moments, Daubechies Wavelet, Haar Wavelet, and Bi-Orthogonal Wavelet, using a genetic algorithm to refine features and then conducting training using an SVM classifier for image retrieval. Garg and Dhiman performed the CBIR

technique using GLCM descriptions to obtain texture image classification with locally rotated binary pattern (LBP) dominant images to extract statistical characteristics combined with classifiers, including supporting vector machines, K nearest neighbors, and decision trees [25]. Multi-feature fusion was used by Niu et al. [26] to develop an image retrieval method that looks for color differences by extracting them using local binary patterns (LBP) after examining the direct relationships between shape and texture features and between color and texture features. In their hybrid approach, Chavda and Goyani [27] used global color histograms and multi-scale local binary patterns as two feature descriptors, and then they performed image retrieval using PCA for dimension reduction and LDA for feature selection. Kayhan suggested a CBIR system based on a mix of weights between color features using quantization color histograms and texture features using modified local environmental differences patterns, local binary patterns, and GLCM [28]. Chu and Liu used a multi-integration feature model to perform CBIR by extracting color and edge data and providing a multi-integration feature histogram [29]. Kugunavar and Prabhakar [30] proposed CBIR of lung images using shape feature extraction with edge histogram (EHD), geometric moment (GM) descriptors, and GLCM for texture features of segmented lung regions using Delaunay triangulation.

Retrieval efficiency is still not able to meet people's needs when only one image feature is retrieved. Thus Zenggang et al. [31] suggested combining the cumulative histogram method with shape features based on Hu moments. Meanwhile, Srivastava et al. use GLCM to search for fabric patterns in the fashion industry. The patterns used are horizontal stripes, vertical stripes, diagonal stripes, checkered patterns, and irregular patterns [32]. Varish [33] proposed a feature fusion scheme that extracted shape features by calculating moments invariant of multi-resolution-based sub-images at various levels. Texture features were extracted using GLCM, and color features were extracted using the probability histogram model method.

Pradhan et al. [34] suggested a way to overcome the ineffectiveness of visual feature-based CBIR by performing feature extraction and combining ROA and non-ROA features. This work extracts image ROA to get the image's semantic meaning based on multi-directional texture and color features based on spatial correlation. Ahmed et al. [35] developed a CBIR for object recognition and retrieval by fusing spatial color features with edge features and then obtained image indexing using bag-of-visual-word and image retrieval with matching schemes. Martey et al. [36] proposed a combination of double color histograms to obtain texture features and color features, namely Stacked Color Histogram and Conventional Color Histogram, which might increase image retrieval accuracy. Fadaei [37] proposed a way to improve CBIR accuracy using the new Dominant Color Descriptor (DCD) method using Canny edges, morphology, and weighting of pixels that are on the edges and not on the edges and tested on three types of datasets Corel-1k (Wang), Corel-10K and Caltech256.

Wang et al. [38] suggested a CBIR for finding the region of the object of concern using the Itti-Koch saliency model. Next, extract the prominent image patterns using a fusion of a multi-feature scheme. Nneji et al. [39] create an image

processing scheme to recognize pneumonia in CXR images using three image feature channels LBP, CECED, and CLAHE, which are processed with a shallow CNN (deep convolutional neural network) by pre-trained inception-V3 and pre-trained MobileNet-V3. The classification results from feature concatenation are more accurate than using only one feature channel. Vharkate and Musande [40] combined CNN Visual Geometry Group (VGG 16, VGG 19, and ResNet) with feature selection using Joint MI to develop a feature extraction method for remote sensing images (Joint Mutual Information). The Relevance Feedback Model (RFM) is used to ensure that search results correspond to user demands. Jardim et al. [41] developed an image retrieval system for the image property industry by implementing multi-phase deep learning and image processing techniques through the use of image signatures to provide an image representation that is close to precise so that plagiarism can be found from trademarks owned by the industry.

The image segmentation approach is used in this work to extract graph features, and the region's adjacency graph is used in the representation. Similarities between two graphs are sought using an inexact graph matching technique that provides error tolerance, in contrast to exact graph matching [42]. This work yielded several contributions, including a framework for image retrieval by combining the graph and low-level feature methods. Another contribution is a retrieval process prototype based on the graph and low-level feature

methods. Image retrieval outcomes are improved when graph and non-graph approaches are combined.

The paper is organized into four sections. The first section is an introduction containing background and reviews of related works. The materials and methods to perform image retrieval, including segmentation and region adjacency graphs, graph edit distances, and low-level feature methods, are explained in the second section. The third section presents the experimental results and discussion. Finally, the final section discusses the conclusion and future work.

II. MATERIALS AND METHOD

Fig. 1 shows a framework utilized as a reference in developing an image retrieval prototype. The retrieval procedure is generally performed using the following algorithm: The user submits a query image, which is then extracted to create a composite feature vector consisting of a graph, color moment, texture, and shape. Extraction is performed on all images in the database to get both graph and non-graph features. Normalization is performed for all features so that the weighting can be determined based on the type of image to be processed. After weighing the features of color, moment, texture, shape, and graph, the similarity value is calculated using a combination of graph and non-graph methods. Finally, when the matching method has been completed, compare the index and obtain the images with the lowest similarity value.

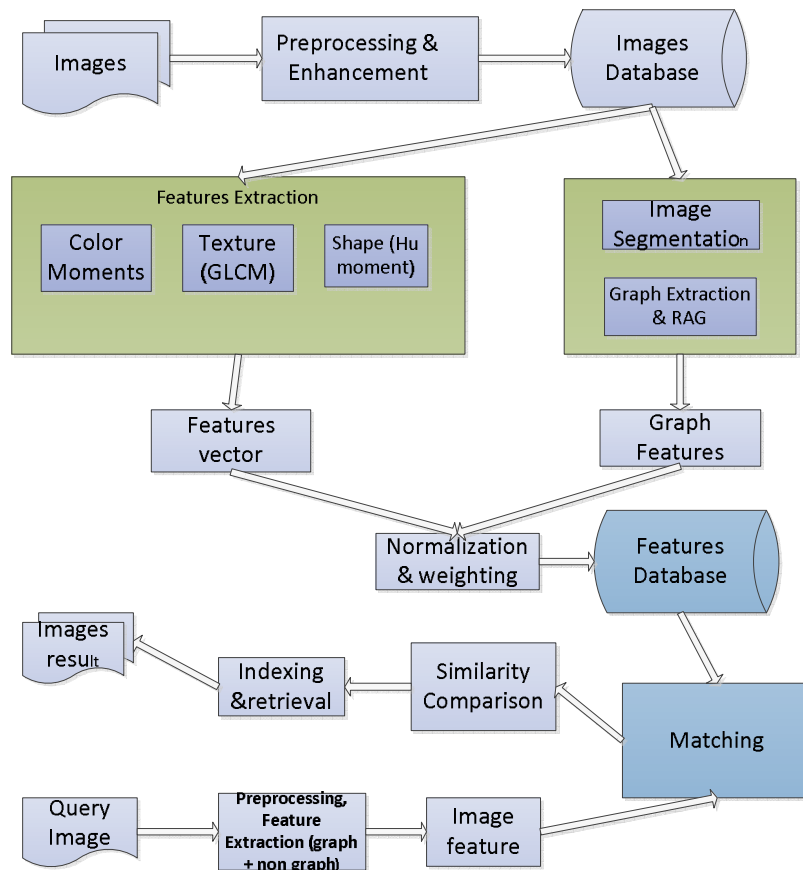


Fig. 1 Image retrieval framework based on a fusion of graph and non-graph methods

Graphs require many resources for data storage and the algorithm's complexity. One option to simplify it is to use segmentation to reduce the number of graph vertices, which

will reduce processing time. The image is segmented into interconnected regions, which are represented using the Region Adjacency Graph (RAG), where vertices indicate

regions and edges reflect relationships between neighboring regions. Each region contains features that may be analyzed to detect similarities between images. The Graph Edit Distance (GED) method of graph matching will be used in the image retrieval procedure to calculate the similarity of the two graphs.

A. Segmentation and Region Adjacency Graph

A graph $G = (V; E)$ is made up of two sets of vertices ($v_i \in V$) and edges (E). E is made up of pairs of elements in V ($e_{ij} \in E$) that are related to the vertices. Image processing using graph methods specifically operates on pixel adjacency graphs where the vertices set is the picture elements set, and edge set is an adjacency relation of the picture elements. A subgraph is a graph whose vertices and edges are subsets of another graph. In other words, a graph whose vertices and edges are all part of a larger graph.

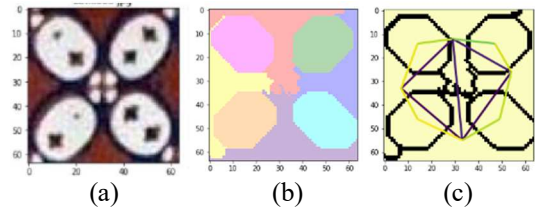


Fig. 2 (a) original image (b) segmented image (c) RAG

The image is divided into several regions or segments that are represented as a graph. The graph is partitioned into some separate connected components, which are the basic principles of segmentation using graphs. Subgraph sets (SG_1, SG_2, \dots, SG_n) will be searched in graph G [43]. The region's centroid will be a node, and the two adjacent regions will be an edge. The representation that uses this method is called the "Region Adjacency Graph" (RAG), as shown in Fig 2. c. There is a reduction in vertices since many pixels in one region will only generate one vertex.

Fig. 3 Feature graph of Fig. 2

Minimum Spanning Tree (MST) using Kruskal's algorithm from Felzenszwalb and Huttenlocher [44] is the segmentation method used in this study. It is called efficient graph-based image segmentation. The spanning tree that has the smallest weight will be the MST. Extraction of image graph features based on the segmentation results in this study produces features such as nodes, areas, centroids, mean color, edges, and edge weights, as shown in Fig. 3.

- Nodes represent regions of image segmentation.
- The centroid is the center point of one region.
- Average color is the average value of RGB pixels in one region.

- The area is the total RGB pixels of one region.
- Edges are pairs of vertices from neighboring regions.
- Weight is the Euclidean distance value of two neighboring regions.

B. Graph Edit Distance (GED)

GED contains methods to find an edit operation set that converts graph G_1 into graph G_2 . Edit cost is used to assess the distortion that occurs in each edit operation such as insert, delete, and substitution [45]. Determining the appropriate edit cost function is a basic requirement when working on the Graph Edit Distance algorithm [46].

Given graphs $G_1 = (V_1; E_1)$, and $G_2 = (V_2; E_2)$. A Graph Edit Distance of G_1 and G_2 is:

$$d(G_1, G_2) = \min_{(ed_1, \dots, ed_k) \in P(G_1, G_2)} \sum_{i=1}^k c(ed_i) \quad (1)$$

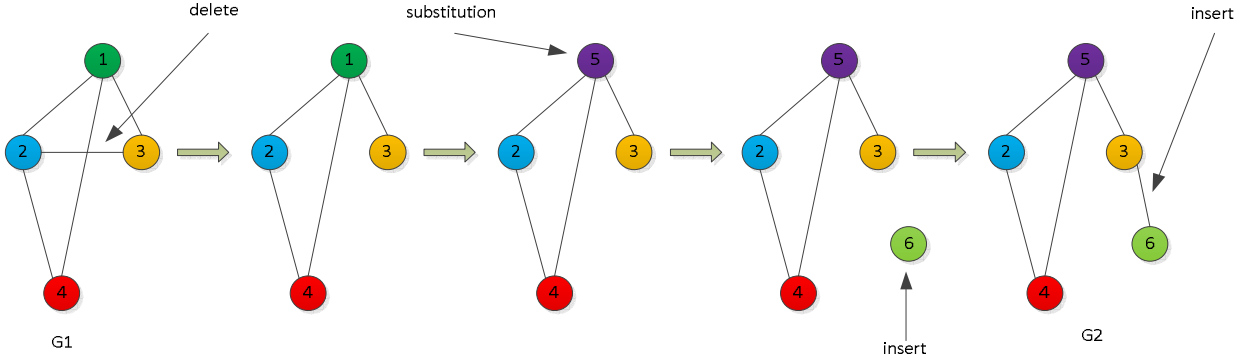


Fig. 4 Example of an edit path between graph G_1 and G_2

For two graphs G_1, G_2 and nonnegative parameters $\alpha, \beta, \gamma, \theta \in R^+ \cup \{0\}$, the cost function is defined for all nodes $u \in V_1$, and $v \in V_2$ for all edges of $p \in E_1$ and $q \in E_2$;

$$c(u \rightarrow \varepsilon) = \gamma \quad (2)$$

$$c(\varepsilon \rightarrow v) = \gamma \quad (3)$$

$$c(u \rightarrow v) = \alpha \cdot \|L(u) - L(v)\| \quad (4)$$

$$c(p \rightarrow \varepsilon) = \theta \quad (5)$$

$$c(\varepsilon \rightarrow p) = \theta \quad (6)$$

$$c(p \rightarrow q) = \beta \cdot \|L(p) - L(q)\| \quad (7)$$

With $L(\cdot)$ notation for labels of elements

C. Low-level feature Methods

Visual features (color, shape, and texture) and semantic features are two things that are often used in the CBIR method. One of the most crucial main features is the visual color feature, and the extraction features of the color are easier compared to other features. In addition, color features do not depend on image transformations such as rotation, scaling, vision, and other deformations, and they have strong resilience.

The mean, variance, and skewness are the first, second, and third-order color moments that effectively and efficiently represent the distribution of the image color. In image retrieval systems, the color moment is commonly utilized.[47]

The three-color moments are defined as follows:

1) *Mean color moment*: the average value of the image color with p_{ij} . is the i -th color channel at the j -th image pixel.

$$E_i = \sum_{j=1}^N \frac{1}{N} p_{ij} \quad (8)$$

2) *Standard Deviation moment*: the variance distribution's square root

$$\sigma_i = \sqrt{\left(\frac{1}{N} \sum_{j=1}^N (p_{ij} - E_i)^2\right)} \quad (9)$$

where $P(G_1; G_2)$ is the edit paths set that change graph G_1 into graph G_2 . $c(ed)$ is the edit cost of the edit operation ed .

3) *Skewness moment*: a measure of the distribution's degree of asymmetry.

$$s_i = \sqrt[3]{\left(\frac{1}{N} \sum_{j=1}^N (p_{ij} - E_i)^3\right)} \quad (10)$$

The shape is one of the basic characteristics in the depiction of objects. Using shape features will increase the accuracy and efficiency of the image retrieval process [48]. Shape characteristics, such as an approximation of objects by a collection of shapes, have been employed in numerous CBIR systems. Hu Moments is a form feature search method that consists of seven values calculated using a central moment whose values are not affected by image transformation [49]. The first six moment values are unchanged concerning translation, rotation, scale, and reflection—the seventh-moment changes to the reflection of the image.

The following formula is used to compute the value of the Hu moment:

$$m_0 = \eta_{20} + \eta_{02} \quad (11)$$

$$m_1 = (\eta_{20} - \eta_{02})^2 + 4\eta_{11}^2 \quad (12)$$

$$m_2 = (\eta_{30} + 3\eta_{12})^2 + (3\eta_{21} - \eta_{03})^2 \quad (13)$$

$$m_3 = (\eta_{30} + \eta_{12})^2 + (\eta_{21} + \eta_{03})^2 \quad (14)$$

$$m_4 = (\eta_{30} - 3\eta_{12})(\eta_{30} + \eta_{12})[(\eta_{30} + \eta_{12})^2 - 3(\eta_{21} + \eta_{03})^2] + (3\eta_{21} - \eta_{03})[3(\eta_{30} + \eta_{12})^2 - (\eta_{21} + \eta_{03})^2] \quad (15)$$

$$m_5 = (\eta_{20} - \eta_{02})[(\eta_{30} + \eta_{12})^2 - (\eta_{21} + \eta_{03})^2 + 4\eta_{11}(\eta_{30} + \eta_{12})(\eta_{21} + \eta_{03})] \quad (16)$$

$$m_6 = (3\eta_{21} - \eta_{03})(\eta_{30} + \eta_{12})[(\eta_{30} + \eta_{12})^2 - 3(\eta_{21} + \eta_{03})^2] + (\eta_{30} - 3\eta_{12})(\eta_{21} + \eta_{03})[3(\eta_{30} + \eta_{12})^2 - (\eta_{21} + \eta_{03})^2] \quad (17)$$

where

$$\eta_{ij} = \frac{\mu_{ij}}{\mu_{00}^{(i+j)/2+1}} \quad (18)$$

which is a normalization of the following central moment:

$$\mu_{ij} = \sum_x \sum_y (x - \bar{x})^i (y - \bar{y})^j I(x, y) \quad (19)$$

\bar{x} and \bar{y} are the centroid coordinates for an area.

A texture feature is a type of feature that is not based on brightness or color. This feature contains surface information and the environment around the image, and the depiction of spatial information from the image can be done quantitatively [50]. The GLCM method is a statistical method for finding image texture features that are calculated using a gray degree distribution. The GLCM approach calculates the amount of contrast, roughness, and granularity of an image region based on the adjacent connection between pixels. Image histograms are used for first-order feature extraction, while a co-occurrence matrix is used for second-order feature extraction. The co-occurrence matrix represents the various orientation directions and spatial distances. [51]. Texture analysis with GLCM has fourteen parameters [52]. Huang et al. [53] found that only four unrelated features of an image could be used to extract the texture features: energy, correlation, contrast, and entropy.

- The second angular moment (energy) shows the uniformity and roughness of the image distribution.

$$f_{ASM} = \sum_{i=0}^{L-1} \sum_{j=0}^{L-1} p_d^2(i, j) \quad (20)$$

- The contrast shows image clarity and texture depth.

$$f_{CON} = \sum_{n=0}^{L-1} n^2 \left\{ \sum_{i=0}^{L-1} \sum_{j=0}^{L-1} p_d(x, y) \right\} \quad (21)$$

- The correlation shows the degree of similarity between components in the row or column direction.

$$f_{COR} = \frac{\sum_{i=0}^{L-1} \sum_{j=0}^{L-1} ij p_d(i, j) - \mu_1 \mu_2}{\sigma_1^2 \sigma_2^2} \quad (22)$$

- Entropy is used to show the randomness of the image texture.

$$f_{ENT} = - \sum_{i=0}^{L-1} \sum_{j=0}^{L-1} p_d(i, j) \log(p_d(i, j)) \quad (23)$$

Texture features with rotational invariance are created by using offset parameters in four directions (0°, 45°, 90°, 135°). Each characteristic index is searched, and its mean and variance are calculated, resulting in a textural feature vector with no relationship to the direction.

III. RESULTS AND DISCUSSION

This section will discuss the suggested system's findings. The suggested system's implementation is written in Python, and the evaluation metric is used to assess the system's performance. Precision is a popular metric for assessing a proposed image retrieval system in which the relevant image serves as the foundation for computations. Precision is defined as the percentage of relevant responses provided by the system among the retrieved occurrences.

$$P = \frac{TP}{TP+FP} \quad (24)$$

P stands for Precision. The relevant images (True Positive) recovered are denoted by TP, while the total number of

images retrieved (True Positive + False Positive) is denoted by TP + FP.

$$AP = \sum_{i=1}^n \frac{P_i}{n} \quad (25)$$

AP stands for Average Precision. The mean accuracy of the class's i images (P_i), where n is the total number of images, is used to calculate AP.

$$MAP = \sum_{j=1}^m \frac{AP_j}{m} \quad (26)$$

MAP is the Mean Average Precision, AP_j is the average precision of the j class image, and m is the total number of classes in the database.

A. Datasets

The image database in this experiment is separated into four categories of datasets: synthetic, batik, COIL-100, and Wang (Table I). There are 200 images in four different classes with 64 x 64-pixel sizes in synthetic, 180 images in three batik variations (Grompol Batik, Parang Batik, and Kawung Batik) with 64 x 64-pixel sizes in Batik, and 100 objects with 7,200 images on a black background in COIL-100. Each object is placed on the table and rotated at 5-degree intervals, resulting in 72 images for each object. Wang's dataset contains 1,000 images divided into ten classes, with sizes 256x386 and 384x256 pixels in JPEG format. Each class has 100 images of Africa, beaches, monuments, buses, dinosaurs, elephants, flowers, horses, mountains, and food.

TABLE I
EXAMPLES OF THE FOUR TYPES OF DATASETS

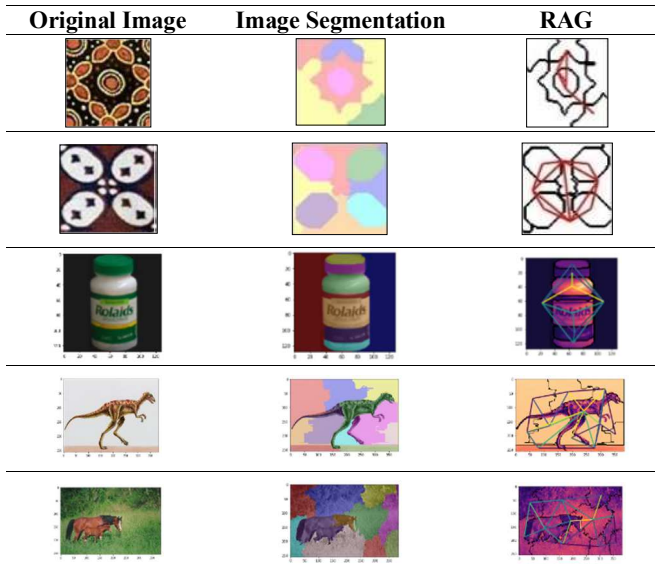
Data set	Images Example
synthetic	
batik	
Coil-100 (Columbia Object Image Library)	
Wang	

B. Segmentation and RAG Results

Images in datasets are segmented into regions and represented using the Region Adjacency Graph (RAG). The number of vertices in each graph is specified between 2 and 15. Table II gives examples of the segmentation and RAG processes for each dataset.

TABLE II
EXAMPLE OF THE SEGMENTATION AND RAG IMAGES

Original Image	Image Segmentation	RAG



In addition, the graph and non-graph feature values are stored in a database table with the following structure: image matrix, image gray, graph label, nodes feature, mean, variance, skewness, glcm, and hu-moments. Table III shows an example of the content of each component.

TABLE III
EXAMPLE OF IMAGE FEATURE CONTENTS

Filename	batik000.jpg	batik001.jpg
image_matrix	[[[193, 97, 57], [178, 86,	[[[220, 84, 60], [215, 85,
image_gray	[[121, 109, 1181...	[[122, 121, 145, 132,
label_graph	[[0, 0, 0, 0, 0, 0,.	[[0, 0, 0, 0, 0, 0,
nodes_feature	[(0, {u'total color': [[(0, {u'total color': [
Mean	[0.093359723894973	[0.093045402347141
variance	[0.411129529138150	[0.412191043205854
Skewness	[0.852782939044841	[0.850153950838359
glcm	[0.696144424879052	[0.688381458592606
Hu Moments	[0.865679376870310	[0.875675324370216

C. Image Retrieval Prototype Model

Giving weights $\omega_1, \omega_2, \omega_3, \omega_4$ to the color moment, Hu Moment, GLCM, and graph methods will give the combined similarity value of the graph method and non-graph method. In this scenario, all feature vector values have been normalized so that the feature values are in the range [0..1].

$$sim = \omega_1 d_{mom}(A, B) + \omega_2 d_{hu}(A, B) + \omega_3 d_{glcm}(A, B) + \omega_4 d_{ged}(A, B) \quad (28)$$

Distance between two feature images measured using Euclidean Distance for both color moment, hu Moment, GLCM, and GED, namely

$$D(A, B) = \sqrt{\sum_{i=0}^n (F_i^B - F_i^A)^2} \quad (29)$$

The algorithm for image retrieval proposed is as follows.

1. Obtain composite feature vectors for moment color, texture, shape, and ged image query.
Look for MeanFeature
Look for VarianceFeature
Look for SkewnessFeature
Look for HuMomentFeature
Look for GLCMFeature
Look for GEDFeature
2. Repeat step 1 for all images to obtain features of all images in the database.
3. Calculate the similarity matrix using the Euclidean distance between the query image and all the images in the database.
Calculate and normalize the mean similarity
Calculate and normalize similarity variance
Calculate and normalize similarity skewness
color moment similarity \leftarrow *average (similarity mean, similarity variance, similarity skewness)*
Calculate and normalize HuMoment similarity
Calculate and normalize GLCM similarity
Calculate and normalize GED similarity
4. Give weight values ($\omega_1, \omega_2, \omega_3, \omega_4$) for the color moment, hu Moment, GLCM, and GED
5. Color moment, Hu Moment, GLCM, and GED features are combined into a single vector for similarity measurements.
Similarity_total \leftarrow $\omega_1 * similarity_moment + \omega_2 * similarity_hu$
 $Moment + \omega_3 * similarity_glcm + \omega_4 * CmpGED$
6. Take the image based on the similarity index.

Fig. 5 Image retrieval process algorithm

Table IV shows the results of image retrieval by using the fusion of the graph method with color moment, Hu Moment, and GLCM. All experiments in these scenarios were conducted using the parameter values of 50% for non-graphs and 50% for graphs. Various weights can also be used as parameter values for retrieval processing by users. Ten distinct types of tests are performed using the graph method, and the CM, HM, and GLCM approaches. Each combination is examined using one of four different types of existing data sets. Some of the test results are shown below.

TABLE IV
EXAMPLE OF FEATURE FUSION WEIGHTS

Method	Weight			
	ω_1	ω_2	ω_3	ω_4
Graph	0	0	0	1
CM + Graph	0.5	0	0	0.5
HM + Graph	0	0.5	0	0.5
GLCM + Graph	0	0	0.5	0.5
CM + HM + Graph	0.25	0.25	0	0.5
CM + GLCM + Graph	0.25	0	0.25	0.5
HM + GLCM + Graph	0	0.25	0.25	0.5
CM + HM +GLCM + Graph	0.17	0.16	0.17	0.5

We will show sample retrieval outcomes from each combination utilizing four different types of data sets. In this scenario, five images will be chosen, one of which has the lowest similarity index value and is the most similar to the query image. The graph method and four combinations of color moments with graphs, GLCM with graphs, Hu Moment with graphs, GLCM with graphs, and combination of color moments, Hu Moment, and GLCM with graphs are chosen as examples (Fig 6,7,8,9).

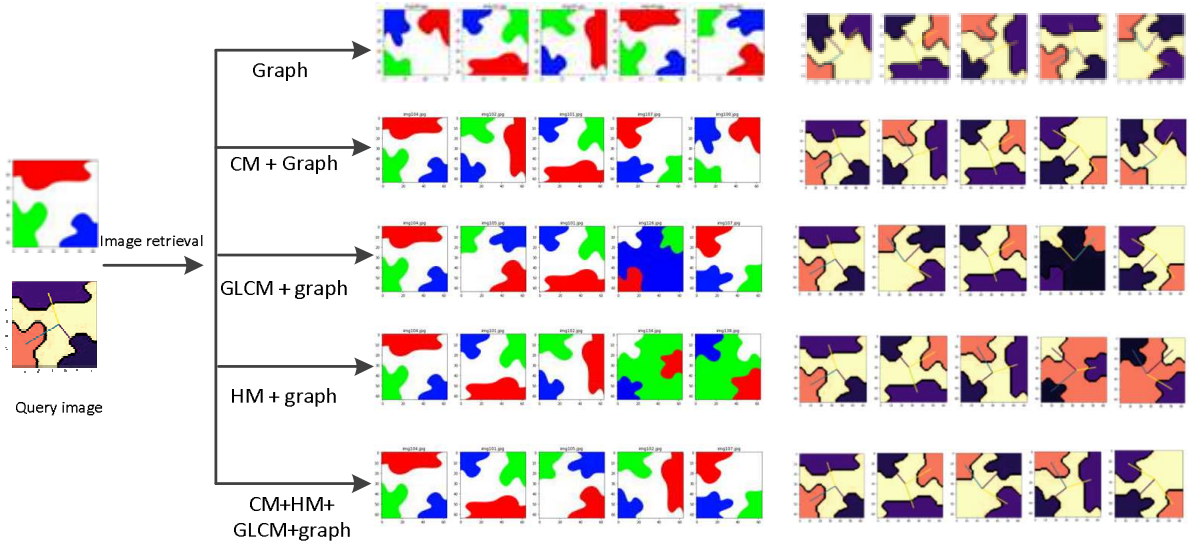


Fig. 6 Query image and image retrieved in synthetic

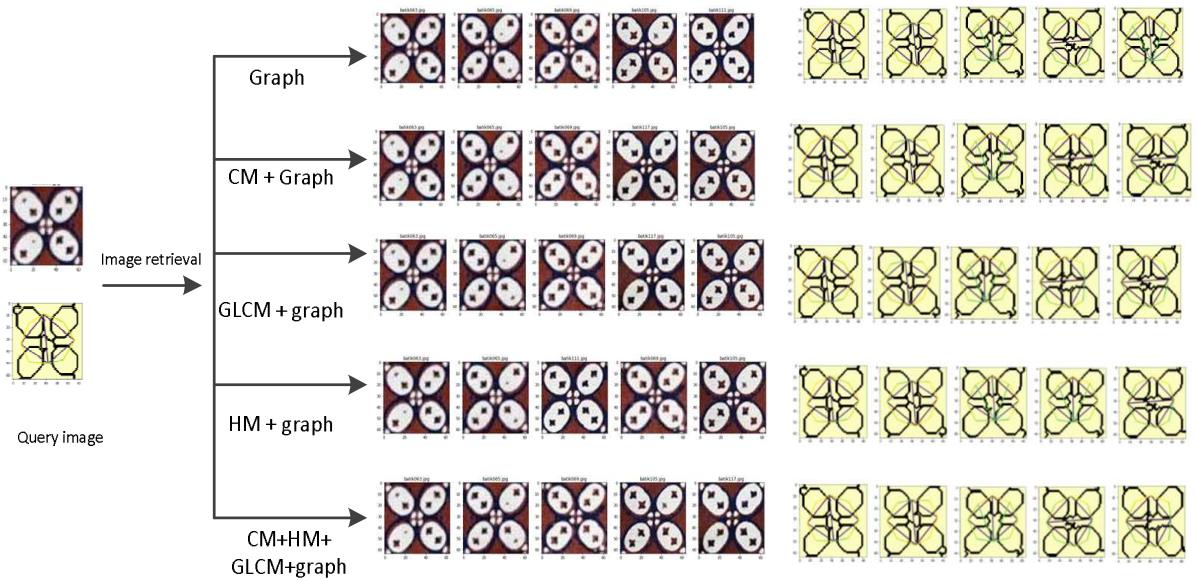


Fig. 7 Query image and image retrieved in batik



Fig. 8 Query image and image retrieved in Coil-100



Fig. 9 Query image and image retrieved in Wang

D. Results Analysis

Table V shows the average precision based on precision value.

TABLE V
MEAN AVERAGE PRECISION (%) OF ALL TYPES OF DATASETS (N=25)

Methods s	Data Set				Average
	Synth	Batik	Coil 100	Wang	
Graph	98.20	82.12	59.02	32.00	67.84
Mean+Graph	93.95	93.48	92.89	68.74	87.27
Mean+Var+Granh	97.59	94.76	95.41	71.06	89.71
CM+Graph	97.33	95.06	94.46	69.20	89.01
GLCM + graph	98.79	88.75	80.09	58.80	81.61
HM + graph	97.86	92.13	68.79	60.12	79.73
CM + GLCM + Graph	98.88	94.89	87.52	68.28	87.39
CM + HM + Graph	97.86	96.97	89.05	60.12	86.00
GLCM + HM + Graph	98.87	94.61	80.54	53.16	81.80
CM + GLCM + HM + Graph	98.52	96.93	88.55	65.16	87.29

CM=Color Moment, GLCM= Grey Scale Co-occurrence Matrix, HM=Hu Moment

Despite having a high precision using only the graph method, the query image is ranked fourth in Fig. 6, example no. 1. After combining the non-graph technique, the query image is in first place. Combining the graph method with the non-graph method enhances the overall accuracy of images retrieved from the image database.

Fig.10 shows a graphical presentation of the MAP of the four categories of data sets. It has been shown that combining the graph method with the color moment, Hu moment, and GLCM methods improves image retrieval accuracy and precision. When using the graph approach alone, our suggested method has a MAP of 67.84 percent, which increases to between 79.73 and 89.7 percent when combined with Color Moment, GLCM, and Hu Moment. This compares to the precision value of Sharma's approach, which ranges between 35 and 67 percent [11], 52.43 percent [12].

RAG will determine the retrieval procedure, which the segmentation findings will significantly influence. Over-segmentation has a major influence on numerous RAG nodes,

causing the matching process to become inaccurate, resulting in a high edit cost value.

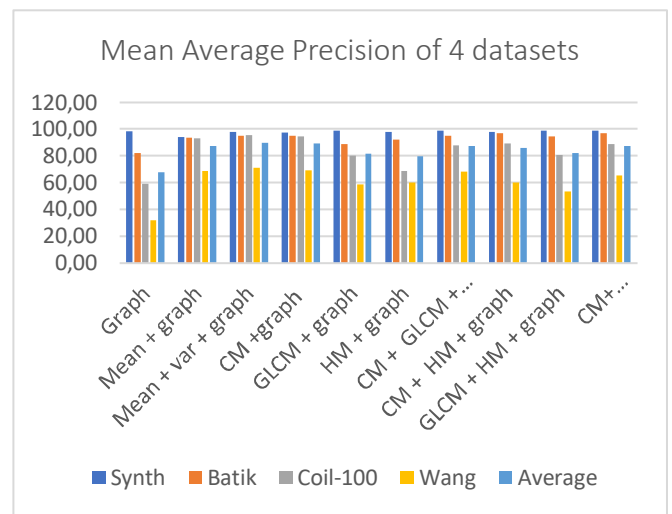


Fig. 10 Mean Average Precision (%) of 4 datasets

Although graph and non-graph fusion techniques have no significant influence on the precision value for Synthetic data, the image capture sequence is more accurate. This also happens with the Batik data. Meanwhile, with Coil-100 and Wang, various over-segmented images arise, producing a very diverse RAG. As a result, the Edit Cost value of GED increases, but the precision value falls. All of this demonstrates that a RAG form with a low variability will offer a high precision value for both graph-based approaches, especially when combined with color moment, GLCM, and Hu Moment methods. Different precision results will be obtained using different parameter settings, depending on the type of image and the emphasis on retrieval priority, whether based on color, shape, or texture.

IV. CONCLUSION

The steps of image retrieval-based fusion of the Graph Method with Color Moments, Hu Moments, and GLCM is illustrated in this paper. Mean color, variance, and skewness are used for color moments, Hu Moments for shapes, and the Gray Level Co-occurrence Matrix (GLCM) for textures. Meanwhile, the graph-based technique compares the similarity of two image graphs based on the Region

Adjacency Graph (RAG) representation using Graph Edit Distance (GED). The graph technique is fused with the non-graph method to get superior retrieval outcomes.

Making RAG is significantly influenced by segmentation results and impacts image retrieval. Over-segmentation creates many nodes in the RAG, leading the matching process to be inaccurate or incur a high edit cost. RAG with low variance will yield a high precision outcome when graph-based techniques are combined with non-graph-based procedures. The next exciting topic to be addressed is the incorporation of semantic components in a graph-based image retrieval technique and the application of machine learning algorithms in its processing.

ACKNOWLEDGMENT

The authors thank BUDI-DN for supporting this research with contract number: PRJ-5777/LPDP.3/2016.

REFERENCES

- [1] A. Latif *et al.*, "Content-based image retrieval and feature extraction: A comprehensive review," *Math. Probl. Eng.*, vol. 2019, 2019, doi: 10.1155/2019/9658350.
- [2] A. Holzinger, B. Malle, and N. Giuliani, "On Graph Extraction from Image Data," in *International Conference on Brain Informatics and Health*, 2014, no. 2003, pp. 552–563.
- [3] L. Brun, P. Foggia, and M. Vento, "Trends in Graph-based Representations for Pattern Recognition," *Pattern Recognit. Lett. Elsevier*, vol. 134, pp. 3–9, 2020, doi: 10.1016/j.patrec.2018.03.016.
- [4] H. Sun, W. Zhou, and M. Fei, "A Survey On Graph Matching In Computer Vision," in *13th International Congress on Image and Signal Processing, BioMedical Engineering and Informatics (CISP-BMEI)*, 2020, pp. 225–230.
- [5] I. Belahyane, M. Mammass, H. Abioui, and A. Idarrou, "Graph-based image retrieval: State of the art," in *9th International Conference on Image and Signal Processing*, 2020, vol. 12119 LNCS, pp. 299–307, doi: 10.1007/978-3-030-51935-3_32.
- [6] S. Chavda and G. Mahesh, "Content-Based Image Retrieval: The State of the Art," *Int. J. Next-Generation Comput.*, vol. 10, no. December, pp. 193–212, 2019.
- [7] I. M. Hameed, S. H. Abdulhussain, and B. M. Mahmmod, "Content-based image retrieval: A review of recent trends," *Cogent Eng.*, vol. 8, no. 1, 2021, doi: 10.1080/23311916.2021.1927469.
- [8] A. K. Nath and A. Wang, "A Survey on Personal Image Retrieval Systems," pp. 1–30, 2020.
- [9] S. Tena, R. Hartanto, and I. Ardiyanto, "Content-based image retrieval for fabric images: A survey," *Indones. J. Electr. Eng. Comput. Sci.*, vol. 23, no. 3, pp. 1861–1872, 2021, doi: 10.11591/ijeecs.v23.i3.pp1861-1872.
- [10] F. D. Wang, N. Xue, Y. Zhang, G. S. Xia, and M. Pelillo, "A functional representation for graph matching," *IEEE Trans. Pattern Anal. Mach. Intell.*, vol. 42, no. 11, pp. 2737–2754, 2020, doi: 10.1109/TPAMI.2019.2919308.
- [11] H. Sharma *et al.*, "Determining similarity in histological images using graph-theoretic description and matching methods for content-based image retrieval in medical diagnostic," *Diagn. Pathol.*, no. October 2012, 2012, doi: 10.1186/1746-1596-7-134.
- [12] A. Kumar, J. Kim, D. Feng, and M. Fulham, "Graph-based retrieval of PET-CT images using vector space embedding," *Proc. CBMS 2013 - 26th IEEE Int. Symp. Comput. Med. Syst.*, pp. 413–416, 2013, doi: 10.1109/CBMS.2013.6627829.
- [13] S. Luo and H. Z. J. Xu, "Matching images based on consistency graph and region adjacency graphs," *Signal, Image Video Process.*, 2016, doi: 10.1007/s11760-016-0987-1.
- [14] D. Valdes-amaro and E. Lopez-prieto, "Image Retrieval using Graphs," in *Future Technologies Conference (FTC) 2017*, 2017, no. November, pp. 1022–1025.
- [15] M. Kashif, G. Raja, and F. Shaikat, "An Efficient Content-Based Image Retrieval System for the Diagnosis of Lung Diseases," *J. Digit. Imaging*, vol. 33, no. 4, pp. 971–987, 2020, doi: 10.1007/s10278-020-00338-w.
- [16] L. P. Valem and D. C. G. Pedronette, "Graph-based selective rank fusion for unsupervised image retrieval," *Pattern Recognit. Lett.*, vol. 135, pp. 82–89, 2020, doi: 10.1016/j.patrec.2020.03.032.
- [17] X. Cortés, D. Conte, and H. Cardot, "Learning edit cost estimation models for graph edit distance ☆," *Pattern Recognit. Lett. Elsevier*, vol. 125, pp. 256–263, 2019, doi: 10.1016/j.patrec.2019.05.001.
- [18] H. Ji-Zhao, G.-H. Liu, and S.-X. Song, "Content-based image retrieval using color volume histograms," *Int. J. Pattern Recognit. Artif. Intell.*, vol. 33, no. 9, p. Article ID 6283987, 2019.
- [19] B. Patel, K. Yadav, and D. Ghosh, "Current Trend and Methodologies of Content-Based Image Retrieval: Survey," 2021, doi: https://doi.org/10.1007/978-981-15-6707-0_64.
- [20] M. K. Alsmadi, "Content-Based Image Retrieval Using Color, Shape and Texture Descriptors and Features," *Arab. J. Sci. Eng.*, vol. 45, no. 4, pp. 3317–3330, 2020, doi: 10.1007/s13369-020-04384-y.
- [21] M. Subramanian, V. Lingamuthu, C. Venkatesan, and S. Perumal, "Content-Based Image Retrieval Using Colour, Gray, Advanced Texture, Shape Features, and Random Forest Classifier with Optimized Particle Swarm Optimization," *Int. J. Biomed. Imaging*, vol. 2022, 2022, doi: 10.1155/2022/3211793.
- [22] S. Singh and S. Batra, "An efficient bi-layer content based image retrieval system," *Multimed. Tools Appl.*, vol. 79, no. 25–26, pp. 17731–17759, 2020, doi: 10.1007/s11042-019-08401-7.
- [23] E. R. Vimina and M. O. Divya, "Maximal multi-channel local binary pattern with colour information for CBIR," *Multimed. Tools Appl.*, vol. 79, no. 35–36, pp. 25357–25377, 2020, doi: 10.1007/s11042-020-09207-8.
- [24] U. A. Khan, A. Javed, and R. Ashraf, "An effective hybrid framework for content based image retrieval (CBIR)," *Multimed. Tools Appl.*, vol. 80, no. 17, pp. 26911–26937, 2021.
- [25] M. Garg and G. Dhiman, "A novel content-based image retrieval approach for classification using GLCM features and texture fused LBP variants," *Neural Comput. Appl.*, vol. 33, no. 4, pp. 1311–1328, 2021.
- [26] D. Niu, X. Zhao, X. Lin, and C. Zhang, "A novel image retrieval method based on multi-features fusion," *Signal Process. Image Commun.*, vol. 87, p. 115911, 2020, doi: 10.1016/j.image.2020.115911.
- [27] S. Chavda and M. Goyani, "2020 Hybrid Approach to Content-Based Image Retrieval Using Modified multi scale LBP and color features.pdf," *SN Comput. Sci. A Springer Nat. J.*, vol. 2020, no. 1, p. 305, 2020, doi: <https://doi.org/10.1007/s42979-020-00321-w>.
- [28] N. Kayhan and S. Fekri-Ershad, "Content based image retrieval based on weighted fusion of texture and color features derived from modified local binary patterns and local neighborhood difference patterns," *Multimed. Tools Appl.*, vol. 80, no. 21, pp. 32763–32790, 2021.
- [29] K. Chu and G. H. Liu, "Image Retrieval Based on a Multi-Integration Features Model," *Math. Probl. Eng.*, vol. 2020, 2020, doi: 10.1155/2020/1461459.
- [30] S. Kugunavar and C. J. Prabhakar, "Content-based medical image retrieval using delaunay triangulation segmentation technique," *J. Inf. Technol. Res.*, vol. 14, no. 2, pp. 48–66, 2021.
- [31] X. Zenggang, T. Zhiwen, and C. Xiaowen, "Research on Image Retrieval Algorithm Based on Combination of Color and Shape Features," *J. Signal Process. Syst.*, vol. 93, no. 2, pp. 139–146, 2019.
- [32] D. Srivastava, B. Rajitha, S. Agarwal, and S. Singh, "Pattern-based image retrieval using GLCM," *Neural Comput. Appl.*, vol. 32, no. 15, pp. 10819–10832, 2020.
- [33] N. Varish, *A modified similarity measurement for image retrieval scheme using fusion of color, texture and shape moments*, vol. 81, no. 15. Multimedia Tools and Applications, 2022.
- [34] J. Pradhan, A. K. Pal, H. Banka, and P. Dansena, "Fusion of region based extracted features for instance-and class-based CBIR applications," *Appl. Soft Comput.*, vol. 102, p. 107063, 2021.
- [35] K. T. Ahmed, S. Ummesafi, and A. Iqbal, "Content based image retrieval using image features information fusion," *Inf. Fusion*, vol. 51, pp. 76–99, 2019.
- [36] E. M. Martey, H. Lei, X. Li, and O. Appiah, "Effective Image Representation using Double Colour Histogram for Content-Based Image Retrieval," *Inform.*, vol. 45, no. 7, pp. 97–105, 2021, doi: 10.31449/inf.v45i7.3715.
- [37] S. Fadaei, "New Dominant Color Descriptor Features Based on Weighting of More Informative Pixels using Suitable Masks for Content-Based Image Retrieval," *Int. J. Eng. Trans. B Appl.*, vol. 35, no. 8, pp. 1457–1467, 2022, doi: 10.5829/IJE.2022.35.08B.01.

- [38] H. Wang, Z. Li, Y. Li, B. Gupta, and C. Choi, "Visual saliency guided complex image retrieval," *Pattern Recognit. Lett. Elsevier*, vol. 130, pp. 64–72, 2020.
- [39] G. U. Nneji, J. Cai, J. Deng, H. N. Monday, E. C. James, and C. C. Ukwuoma, "Multi-Channel Based Image Processing Scheme for Pneumonia Identification," *Diagnostics*, vol. 12, no. 2, pp. 1–26, 2022, doi: 10.3390/diagnostics12020325.
- [40] M. N. Vharkate and V. B. Musande, "Fusion Based Feature Extraction and Optimal Feature Selection in Remote Sensing Image Retrieval," *Multimed. Tools Appl.*, vol. 81, no. 22, pp. 31787–31814, 2022, doi: 10.1007/s11042-022-11997-y.
- [41] S. Jardim, J. António, C. Mora, and A. Almeida, "A Novel Trademark Image Retrieval System Based on Multi-Feature Extraction and Deep Networks," *J. Imaging*, vol. 8, no. 9, 2022, doi: 10.3390/jimaging8090238.
- [42] C. Oyarzun Laura, S. Wesarg, and G. Sakas, "Graph matching survey for medical imaging: On the way to deep learning," *Methods*, no. July 2021, 2021, doi: 10.1016/j.ymeth.2021.06.008.
- [43] K. S. Camilus and V. K. Govindan, "A Review on Graph Based Segmentation," *Int. J. Image, Graph. Signal Process.*, vol. 4, no. June, pp. 1–13, 2012, doi: 10.5815/ijigsp.2012.05.01.
- [44] P. F. Felzenszwalb and D. P. Huttenlocher, "Efficient graph-based image segmentation," *Int. J. Comput. Vis.*, vol. 59, no. 2, pp. 167–181, 2004, doi: 10.1023/B:VISI.0000022288.19776.77.
- [45] E. Rica, S. Álvarez, and F. Serratos, "On-line learning the graph edit distance costs," *Pattern Recognit. Lett.*, vol. 146, pp. 55–62, 2021, doi: 10.1016/j.patrec.2021.02.019.
- [46] F. Serratos, "A general model to define the substitution, insertion and deletion graph edit costs based on an embedded space," *Pattern Recognit. Lett.*, vol. 138, pp. 115–122, 2020, doi: 10.1016/j.patrec.2020.07.010.
- [47] R. M. Bommisetty, O. Prakash, and A. Khare, *Keyframe extraction using Pearson correlation coefficient and color moments*, vol. 26, no. 3. Springer Berlin Heidelberg, 2020.
- [48] G. Xie, B. Guo, Z. Huang, Y. Zheng, and Y. Yan, "Combination of Dominant Color Descriptor and Hu Moments in Consistent Zone for Content Based Image Retrieval," *IEEE Access*, vol. 8, pp. 146284–146299, 2020, doi: 10.1109/ACCESS.2020.3015285.
- [49] Z. Huang and J. Leng, "Analysis of Hu's moment invariants on image scaling and rotation," *ICCET 2010 - 2010 Int. Conf. Comput. Eng. Technol. Proc.*, vol. 7, no. May 2010, 2010, doi: 10.1109/ICCET.2010.5485542.
- [50] A. Humeau-Heurtier, "Texture feature extraction methods: A survey," *IEEE Access*, vol. 7, no. c, pp. 8975–9000, 2019, doi: 10.1109/ACCESS.2018.2890743.
- [51] A. Eleyan and H. Demirel, "Co-occurrence matrix and its statistical features as a new approach for face Recognition," *Turkish J. Electr. Eng. Comput. Sci.*, vol. 19, no. 1, 2011, doi: 10.3906/elk-0906-27.
- [52] Haralick, R.M and K. Shanmugam, "Texture features for image classification," *EEETrans. Syst. Man Cybern. SMC*, vol. 3, no. 6, pp. 610–621, 1973.
- [53] M. Huang, H. Shu, Y. Ma, and Q. Gong, "Content-based image retrieval technology using multi-feature fusion," *Opt. - Int. J. Light Electron Opt.*, vol. 126, no. 19, pp. 2144–2148, 2015, doi: 10.1016/j.ijleo.2015.05.095.